the halide cores of the reductants as the rate-determining step of reactions 1.[5a,11,13-15]

When X = Br, 10^2k_T for reaction 1 with N = *N*,*N*-diethylnicotinamide is 58 M^{-1} s^{-1} at 25 °C in nitrobenzene.[5a] Rate constant k_9 for the oxidation of $[NCuI]_4Y$ in reaction 8 is lower by a factor of ca. 5.[20] The proposed core structure of $[NCuI]_4Y$ (Scheme I) contains bridging catecholate on one face that would seriously impede O_2 insertion through that face. Since the products of reactions 8 are mono(μ-oxo)copper(II) complexes, insertion of O_2 through the halide cores of $[NCuX]_4Y$ is unnecessary for their formation.[20] In line with this reasoning, we find that the data for rate law 9 and the corresponding data for second-order oxidation of $[NCuBr]_4Y$ by dioxygen[20] do not fit the linear activation parameter correlation in Figure 6.

It has been proposed that reactions 9 proceed via the alternative mechanism shown in Scheme I.[20] Assumption of a steady state for respective intermediates II (X = Br, I) gives eqs 14 and 15.

$$[II] = k_{14}[[NCuX]_4Y][O_2]/(k_{-14} + k_{15}[[NCuX]_4Y]) \quad (14)$$

$$d[[NCuX]_4Y(O)]/dt = 2k_{15}[[NCuX]_4Y][II] = 2k_{14}k_{15}[[NCuX]_4Y]^2[O_2]/(k_{-14} + k_{15}[[NCuX]_4Y]) \quad (15)$$

Equation 15 has two obvious limits. One limit, $k_{-14} \ll k_{15}[[NCuX]_4Y]$, gives eq 16, which has the same second-order form as rate law 9, with $k_9 = 2k_{14}$. This situation corresponds

$$d[[NCuX]_4Y(O)]/dt = 2k_{14}[[NCuX]_4Y][O_2] \quad (16)$$

to rate-determining formation of "peroxocopper" intermediate II and its much faster reduction by a second mole of $[NCuX]_4Y$.[20] It is a reasonable conclusion because the copper(I) centers of $[NCuX]_4Y$ should be especially stabilized by X = Br and I.[19]

Assumption of a similar limiting mechanism for the oxidation of $[LCuI]_2$ complexes by dioxygen in nitrobenzene leads to the same conclusion: the rate-determining step is the reversible oxidation of one molecule of $[LCuI]_2$ by one molecule of O_2 to give some sort of "peroxocopper(II)" intermediate $[LCuI]_2(O_2)$. This is again a reasonable conclusion because copper(I) is especially stabilized by iodide.[19] We imagine that $[LCuI]_2(O_2)$ has the same sort of "peroxide" geometry as that shown in Scheme I because of the known[7] short Cu···Cu separations in $[LCuI]_2$. In any event, this intermediate is rapidly reduced by excess $[LCuI]_2$.[26]

The question now is why the kinetic data for rate law 13 fit the very good correlation of activation parameters for insertion-limited[2g,5a,11,14,15] copper(I) oxidation reactions in Figure 6. Is it possible that oxidations of $[LCuI]_2$ by O_2 require slow insertion of the dioxygen molecule through the planar[7,12] face Cu(I,I)Cu between the copper(I) centers? Lower second-order rate constant k_{13} on changing L from TEED to TMED (Table IV) could be due to a decrease in the Cu···Cu separation from 2.66 to 2.58 Å in the respective reductants $[LCuI]_2$.[7] A decrease in the width of the $[LCuI]_2$ core would slow down a penetration reaction. In any event, the negative activation entropies for rate law 13 (Table IV) indicate an associative slow step for $[LCuI]_2$ oxidation by dioxygen.

Acknowledgment. This work was supported by Grants INT-8715384, INT-8918985, and CHE-8717556 from the National Science Foundation, which are gratefully acknowledged. We thank Drs. Arthur Heiss and Ralph Weber of Bruker Instruments for help with the EPR measurements and Noralie Barnett and Amro El-Maradne for technical assistance.

Supplementary Material Available: Table III, giving kinetic data for the oxidation of dimeric iodocopper(I) complexes $[LCuI]_2$ by dioxygen in nitrobenzene (1 page). Ordering information is given on any current masthead page.

(26) A reviewer suggested that the intermediates in $[LCuI]_2/O_2$ reactions could be hypoiodito complexes $[LCu(IO)]_2$ rather than peroxo complexes $[LCuI]_2O_2$. We know of no precedent for amine(hypoiodito)copper(II) complexes.

Contribution from the Department of Chemistry, University of Manchester, Manchester M13 9PL, England

Electron Spin Resonance Studies of "FeO_6" Tris Chelate Complexes: Models for the Effects of Zero-Field Splitting in Distorted $S = {}^5/_2$ Spin Systems

David Collison* and Anne K. Powell[1]

Received May 12, 1988

The electron spin resonance (ESR) spectra of a series of substituted malonato and oxalato, high-spin, tris chelate complexes of iron(III) have been determined at both X- and Q-band frequencies for powdered polycrystalline samples in the temperature range 300–77 K. A diverse range of frequency-dependent spectra are reported, and these spectra are interpreted by using a spectrum simulation program based on matrix diagonalization methods for a general spin Hamiltonian incorporating electronic Zeeman and zero-field splitting terms. Data are presented that serve to form a library of spectra for octahedrally distorted $S = {}^5/_2$ spin systems. The observed spectra of these tris-chelate complexes vary with counterion, substituent on the ligand, and degree of hydration in an unpredictable manner.

Introduction

The $\{Fe^{III}O_6\}$ moiety in coordination complexes may be used as an active-site model[2] for some aspects of iron(III) chemistry in certain biological systems as well as an example of inherent photochemical reactivity.[3] Electron spin resonance (ESR) spectroscopy may be a sensitive probe of the metal site geometry in such circumstances. Photosensitive iron(III) complexes have been much used in imaging systems;[4] for example tris(oxalato)ferrate(III), $[Fe(ox)_3]^{3-}$, has been used in non-silver photographic printing processes such as the platinotype and blueprint methods. During the course of our investigations of the photoactivity of a range of dicarboxylato complexes of iron(III), we discovered that the details of the electronic structure, as assessed by ESR spectroscopy, of a seemingly closely related set of such complexes displayed an unexpected variety. A most sensitive spectroscopic probe of such systems comes from the application of multifre-

(1) Present address: School of Chemical Sciences, University of East Anglia, Norwich NR4 7TJ, U.K.
(2) (a) Raymond, K. N.; Isied, S. S.; Brown, L. D.; Fronczek, F. R.; Nibert, J. H. *J. Am. Chem. Soc.* **1976**, *98*, 1766. (b) Kiggen, W.; Vogtle, F. *Angew. Chem., Int. Ed. Engl.* **1984**, *23*, 714.
(3) (a) *Photochemistry of Coordination Compounds*, Balzani, V., Carassiti, V., Eds.; Academic Press: London, 1970. (b) Wehry, E. L. *Q. Rev., Chem. Soc.* **1967**, *21*, 213. (c) Adamson, A. W.; Waltz, W. L.; Zinato, E.; Watts, D. W.; Fleischauer, P. D.; Lindholm, R. D. *Chem. Rev.* **1968**, *68*, 541.
(4) Kosar, J. *Light Sensitive Systems*; Wiley: New York, 1965.
(5) *Metal Ions in Biological Systems*; Sigel, H., Ed.; Marcel Dekker Inc.: New York, 1978; Vol. 7.

0020-1669/90/1329-4735$02.50/0

quency ESR spectroscopy. Additionally, ESR spectroscopy has been used increasingly as a probe of the iron(III) site(s) in biological systems.[2,6-9] The strong affinity of iron(III) for oxygen donor ligands is well-known,[10,11] and accordingly "FeO_6" centers are important in iron storage[12] and transport[13] proteins. Thus a link is formed between the photochemical and bioinorganic areas in these tris(carboxylato) complexes. The ESR spectra of the series of oxalato salts of iron(III), hexamminecobalt salts of tris(malonato) derivatives of general formula $[Co(NH_3)_6][Fe\{CR^1R^2(COO)_2\}]\cdot nH_2O$, and other related carboxylato complexes of iron prompted us to try to find a way of rationalizing the wide range of spectral patterns we recorded. Characteristic ESR spectra of high-spin iron(III) complexes have been obtained by various workers.[14-16] Two distinct approaches may be employed in the interpretation of the ESR spectra derived from high-spin iron(III) complexes, namely: (i) spectral simulation; (ii) comparison with model complexes. These two will be treated separately.

(i) Spectral Simulation. The analyses of ESR spectra of iron(III) arising from the dilution of the Fe^{3+} ion in various diamagnetic host lattices by single-crystal methods are well documented.[17] In general, such studies involve the interpretation of narrow-line spectra and require detailed crystallographic information in order to obtain the values of the ESR parameters. All simulation methods require the use of a general spin Hamiltonian[18] (eq 1).

$$\mathbf{H} = \beta_e B\cdot\tilde{g}\cdot\hat{S} + \sum_{n=2,4}\sum_{m=-n}^{n} C_{nm}O_n^m(\hat{S}) \qquad (1)$$

This expression can be recast in terms of other parameters:

$$\mathbf{H} = \beta_e(B\cdot\tilde{g}\cdot\hat{S}) + \frac{D}{3}O_2^0 + EO_2^2 + \left(\frac{a}{120} + \frac{F}{180}\right)O_4^0 + \frac{H}{3}O_4^2 + \left(\frac{a}{24} + 2G\right)O_4^4$$

for $S = {}^5/_2$ where β_e = electronic Bohr magneton, B is the applied magnetic field and C and O the coefficients and operators allowed for a spin sextet. In this way the Fe^{3+} ion has been used as a probe of the behavior of ionic sites in lattices to monitor the effects of temperature variation,[19] stress,[20] phase transitions,[21] dehydration of crystals,[22] motions of water molecules,[23] and photochemical processes[24] by comparison with crystal structures.

(ii) Model Complexes. Only three "FeO_6" complexes have been studied in detail by magnetic methods. These are $[Fe(C_2O_2S_2)_3]^{3-}$[25] and $[Fe(C_2O_4)_3]^{3-}$[26] studied by ESR, and $[Fe(C_2O_4)_3]^{3-}$ and $[Fe(acac)_3]$, where acac = pentane-2,4-dionate, studied by magnetic anisotropy measurements.[27] The latter neither allowed an accurate determination of the magnitude of the zero-field splitting nor took into account the effects due to rhombic distortion at the metal.

The method chosen to analyze the ESR spectrum measured for any particular system containing high-spin iron(III) depends on the assumed relative magnitudes of the zero-field splitting parameter, D, and the microwave frequency (ν) used in measuring the spectrum. Closed form expressions[28-31] giving resonance positions may be derived from the spin Hamiltonian of eq 1 (or a truncated form) under certain specific conditions, viz. $D \gg h\nu$ or $h\nu \gg D$, by using the methods of perturbation theory and/or special directions of the applied magnetic field relative to the molecular axes. The methods of analysis may be simplified in many cases by acquiring single-crystal data. However, in general, where single crystals may not be available, when the relative magnitudes of D and the incident microwave energy, ν, are not known and only relatively small quantities of sample are accessible, even the identification of a system as high-spin iron(III) by magnetic methods may be difficult. Under the circumstances where $D \approx h\nu$, spectrum simulation procedures based on perturbation theory[29,32] or the eigenfield method[28,33] break down and it is necessary to use matrix-diagonalization methods. This exact diagonalization approach may be limited if the computational time becomes prohibitively long (to eliminate spectral artifacts[34]) or if it is necessary to restrict the simulations to the high-symmetry (axial) case.[25] However, devices designed to speed up such calculations[35] are often to the detriment of the final convoluted powder spectrum, so that while the positions of features are often accurately reproduced, their band shapes and relative intensities may lead to large discrepancies between the experimental and simulated spectra and hence an erroneous interpretation of the observed spectrum. Such methods are valuable aids to spectrum interpretation as long as their limitations are recognized. Two matrix-diagonalization methods that do not include the use of "effective" parameters, which are therefore are computationally slow, have been reported.[36,37]

From the foregoing discussion, it may be seen that the interpretation of the ESR spectra of $S = {}^5/_2$ systems is difficult, yet Fe^{III} arises in a wide variety of chemical and biological situations. We wish to present here a unified approach to this problem in which the results of calculation via matrix diagonalization over all orientations of the magnetic field with respect to the **g** tensor axes for the general case are compared with the experimental spectra obtained at both X- and Q-band frequencies in the temperature range 77–300 K for a series of "FeO_6" complexes whose

(6) Aasa, R.; Aisen, P. *J. Biol. Chem.* **1968**, *243*, 2399.
(7) Burch, J. H. In *Metalloproteins. Topics in Molecular and Structural Biology*; Harrison, P. M., Ed.; Macmillan Press: London, 1985; Vol. 7, Part II, pp 203, 246.
(8) Weir, M. P.; Peters, T. J.; Gibson, J. F. *Biochem. Biophys. Acta* **1985**, *828*, 298.
(9) Thompson, C. P.; McCarty, B. M.; Chasteen, N. D. *Biochem. Biophys. Acta* **1986**, *870*, 530.
(10) Cotton, F. A.; Wilkinson, G. *Advanced Inorganic Chemistry*; Wiley-Interscience: New York, 1980; p 759.
(11) Greenwood, N. N.; Earnshaw, A. *Chemistry of the Elements*; Pergamon Press: Oxford, 1984; p 1265.
(12) Theil, E. C. *Adv. Inorg. Biochem.* **1983**, *5*, 1. Rice, D. W. *Adv. Inorg. Biochem.* **1983**, *5*, 39.
(13) Huheey, J. E. *Inorganic Chemistry—Principles of Structure and Reactivity*; Harper and Row: New York, 1983; p 896.
(14) Sugiura, Y.; Mino, Y.; Iwashita, T.; Namoto, K. *J. Am. Chem. Soc.* **1985**, *107*, 4669.
(15) Pecoraro, V. L.; Wong, G. B.; Kent, T. A.; Raymond, K. N. *J. Am. Chem. Soc.* **1983**, *105*, 4617.
(16) Berry, K. J.; Clark, P. E.; Murray, K. S.; Raiston, C. L.; White, A. M. *Inorg. Chem.* **1983**, *22*, 3928.
(17) See, for example: (a) McGavin, D. G.; Tennant, W. C. *J. Magn. Reson.* **1985**, *61*, 321. (b) Gaite, J. M.; Bulka, G. R.; Husanova, N. M.; Nizamutdinov, N. M.; Vinokurov, V. M. *J. Chem. Phys.* **1985**, *82*, 4358.
(18) Abragam, A.; Bleaney, B. *Electron Paramagnetic Resonance of Transition Ions*; Clarendon Press: Oxford, England, 1970; p 139ff.
(19) (a) Hendrickson, D. N.; Haddad, M. S.; Federer, W. D.; Lynch, M. W. *Coord. Chem.* **1980**, *21*, 75. (b) Timken, M. D.; Abdel-Mawgoud, A. M.; Hendrickson, D. N. *Inorg. Chem.* **1986**, *25*, 160.
(20) Lukin, S. N.; Nakashidze, G. A.; Teslya, O. P.; Tsintsadze, G. A. *Fiz. Tverd. Tela (Leningrad)* **1982**, *24*, 303.
(21) Leble, A.; Rousseau, J. J.; Fayet, J. C.; Pannetier, J.; Fourquet, J. L.; De Pape, R. *Phys. Status Solidi A* **1982**, *69*, 249.
(22) Karimova, A. F. *Teor. Eksp. Khim.* **1981**, *17*, 268.
(23) Golovin, A. V.; Krivuruchko, O. P.; Buyanov, R. A.; Zolotovskii, B. P. *Izv. Sib. Otd. Akad. Nauk SSR, Ser. Khim. Nauk.* **1981**, 70.
(24) Petrak, P. Z.; Spees, S. T. *Abstracts of Papers*; 153rd National Meeting of the American Chemical Society, Miami Beach, FL, April 1967.
(25) Sweeney, W. V.; Coucouvanis, D.; Coffman, R. E. *J. Chem. Phys.* **1973**, *59*, 369.
(26) Doetschman, D. C.; McCool, B. J. *Chem. Phys.* **1975**, *8*, 1.
(27) Gerloch, M.; Lewis, J.; Slade, R. C. *J. Chem. Soc. A* **1969**, 1422.
(28) Scullane, M. I.; White, L. K.; Chasteen, N. D. *J. Magn. Reson.* **1982**, *47*, 383.
(29) Aasa, R. *J. Chem. Phys.* **1970**, *52*, 3919.
(30) Golding, R. M.; Singhasuwich, T.; Tennant, W. C. *Mol. Phys.* **1977**, *34*, 1343.
(31) Pilbrow, J. *J. Magn. Reson.* **1978**, *31*, 479.
(32) Purans, J.; Kliava, J.; Milliere, I. *Phys. Status Solidi A* **1979**, *56*, K25.
(33) Belford, G. G.; Belford, G. L.; Burkhalter, J. F. *J. Magn. Reson.* **1973**, *11*, 251.
(34) Oosterhuis, W. T. *Struct. Bonding* **1974**, *20*, 59.
(35) (a) McGavin, D. G.; Tennant, W. C. *J. Magn. Reson.* **1985**, *62*, 357. (b) Nettar, D.; Villafranca, J. J. *J. Magn. Reson.* **1985**, *64*, 61.
(36) (a) Dowsing, R. D.; Gibson, J. F. *J. Chem. Phys.* **1969**, *50*, 294. (b) Dowsing, R. D.; Ingram, D. J. E. *J. Magn. Reson.* **1969**, *1*, 517.
(37) Collison, D.; Mabbs, F. E. *J. Chem. Soc., Dalton Trans.* **1982**, 1565.

structures are known or implied from single-crystal X-ray studies. The major purpose of this paper is to report, in a pictorial manner, the wide variety of ESR spectra that can be produced from $S = {}^5/_2$ spin systems and for which there is *no* change in ligand donor atom type. Despite the limitations of our approach, this is the first time that a library of spectral types for high-spin ferric systems has been presented. The data reported herein may be used, in conjunction with the resonance field diagrams already in the literature (see for example ref 29), if necessary, to allow a more facile interpretation of Fe(III) ESR spectra. We illustrate the use of the method by estimating parameters for a series of "FeO_6" complexes.

Experimental Section

Preparation of Compounds. Because of the reported[3] photosensitivity of many aqueous solutions of iron(III) with carboxylic acids, reactions and crystallizations were performed with the exclusion of direct sunlight and any light sources known to produce significant amounts of soft ultraviolet and blue light.

Reactions were carried out with *no* precautions to exclude oxygen, and all products were stable to handling and storage in air. Metal salts, oxalate salts, and oxalic acid were obtained from BDH Chemicals Ltd. Malonic acids $[Cr^1R^2(COOH)_2]$, the substituted diamines *N,N,N',N'*-tetramethylethylenediamine (TMED) and *N,N'*-dimethylpiperazine (DMPIP), and ketovaleric and hydroxybutyric acids were obtained from Aldrich Chemical Co. Hexamminecobalt chloride was prepared by using the method of Brauer.[38] All reagents were used as obtained without further purification. Analyses were performed by the Microanalysis Laboratory of the Chemistry Department of the University of Manchester.

Tris(oxalato)ferrate(III) Complexes. The preparation of pure complexes may be complicated by coprecipitation of the ligand (or one of its salts) and hydrolysis of the complex, which tends to occur in aqueous solutions.

Method 1. Following the procedure of Bailar and Jones,[39] we prepared barium oxalate by mixing equal volumes of barium chloride and sodium or potassium oxalate, from which barium oxalate precipitated immediately. A mixture of barium oxalate (3 equiv), aqueous ferric sulfate (1 equiv), and aqueous potassium oxalate (3 equiv) was left to digest on a steam bath for 2 h and then filtered and the green solution left to crystallize.

Method 2. In the general method after Calvert and Pitts,[40] a solution containing ferric chloride (1 equiv) and the appropriate oxalate salt (3 equiv) were heated together. Concentrated solutions (ca. 1.5 M) were used from which the product sometimes began to crystallize when still hot.

Method 3. The tris(oxalato)ferrate(III) complex was generated in solution by the addition of an aqueous solution of sodium oxalate (3 equiv) to a solution of iron(III) chloride (1 equiv). An appropriate quantity of a large counter cation such as hexamminecobalt chloride or $DMPIPH_2^{2+}$ in aqueous solution was then added and the mixture left to crystallize.

Method 4. There is a method of preparing $(NH_4)_3[Fe(ox)_3]\cdot 3H_2O$ (ox = oxalate) which is peculiar to this salt.[41] Iron(III) nitrate enneahydrate was finely ground, and 3 equiv of ground ammonium oxalate were added. The two powders were thoroughly mixed whereupon the water of crystallization of the nitrate was sufficient to form a syrupy solution of the green ammonium tris(oxalato)ferrate(III) salt. The syrup was transferred to a suitable vessel and was warmed slightly under a hot-water tap to maintain a solution as the vessel becomes quite cold. The product was isolated by careful addition of excess methanol in which ammonium nitrate is soluble but the complex is not.

Satisfactory total elemental analyses (excluding oxygen) were obtained for the following oxalato complexes with the method of preparation given in parentheses: $K_3[Fe(ox)_3]\cdot 3H_2O$ (method 1); $[Co(NH_3)_6][Fe(ox)_3]\cdot 2H_2O$ (method 3); $Na_3[Fe(ox)_3]\cdot 4.5H_2O$ (method 2); $[NH_4]_3[Fe(ox)_3]\cdot 4.5H_2O$, form I (method 2); $[NH_4]_3[Fe(ox)_3]\cdot 4.5H_2O$, form II (method 4); $[TMEDH_2]_3[Fe(ox)_3]_2\cdot 4H_2O$ (method 3); $[DMPIPH_2]_3[Fe(ox)_3]_2\cdot 8H_2O$ (method 3).

Tris(malonato)ferrate(III) Complexes: $[Fe\{CR^1R^2(COO)_2\}_3]^{3-}$. $K_3[Fe(mal)_3]\cdot H_2O$ (mal = malonate, where $R^1 = R^2 = H$) was prepared by a modification of the method of Scholz.[42]

A solution of iron(III) chloride ($FeCl_3$; 1.62 g, 10 mmol) in water (10 mL) was treated with a solution of malonic acid (3.12 g, 30 mmol) and potassium hydroxide (3.36 g, 60 mmol) in water (20 mL). Green crystals of the tripotassium salt formed over a period of days.

The preparative method for unsubstituted malonic acid given below was followed for the other acids.

Method 5. The tris(malonato)ferrate(III) ion was generated in aqueous solution by mixing a solution of sodium hydroxide (2.40 g, 60 mmol) and malonic acid (3.12 g, 30 mmol) in water (50 mL) with a solution of iron(III) chloride ($FeCl_3$; 1.62 g, 10 mmol) in water (50 mL). An aqueous solution of hexamminecobalt chloride (100 mL of a 100-mmol solution) was added to the green solution and the volume made up to 250 mL. Orange crystals of hexamminecobalt tris(malonato)-ferrate(III) pentahydrate formed over 36 h.

Satisfactory total elemental analyses (excluding oxygen) were obtained for the following malonato complexes as their hexamminecobalt salts of general formula $[Co(NH_3)_6][Fe\{CR^1R^2(COO)_2\}_3]\cdot nH_2O$, with the number of molecules of water of crystallization given in parentheses: $[Fe\{CH_2(COO)_2\}_3]^{3-}$ ($n = 5$); $[Fe\{CHCH_3(COO)_2\}_3]^{3-}$ ($n = 6$); $[Fe\{C(CH_3)_2(COO)_2\}_3]^{3-}$ ($n = 0$); $[Fe\{CHC_2H_5(COO)_2\}_3]^{3-}$ ($n = 6$); $[Fe\{C(C_2H_5)_2(COO)_2\}_3]^{3-}$ ($n = 4.5$).

Iron(III) Tris(ketovalerate). An aqueous solution of the monosodium salt of α-ketovaleric acid (0.06 mol = 0.84 g of the monohydrate in 6 cm^3 of water) was added to an aqueous solution of iron(III) chloride (0.02 mol = 0.32 g of the anhydrous salt in 2 cm^3 of water). A red powder precipitated after 3 days.

Anal. Calcd for $Fe(C_5H_7O_3)_3\cdot 2H_2O$: C, 41.2; H, 5.8; Fe, 12.8. Found: C, 41.7; H, 5.4; Fe, 12.8.

Iron(III) Tris(hydroxybutyrate). α-Hydroxybutyric acid (1.56 g) was dissolved in water (20 cm^3), and an aqueous solution (10 cm^3) of iron(III) chloride (0.81 g of $FeCl_3$) was added to give a brown solution. A green microcrystalline solid formed over a week which fits the required formulation for a tris chelate.

Anal. Calcd for $[Fe(CH_3CH_2CH(OH)COO)_3]$: C, 39.51; H, 5.8; Fe, 15.3. Found: C, 38.7; H, 5.7; Fe, 14.8.

Iron(III) Tris(acetylacetonate). $[Fe(acac)_3]$ was prepared by using literature methods,[27] and satisfactory elemental analyses were obtained.

All the above compounds were identified by a combination of microanalytical and infrared measurements using structurally characterized complexes as references (see later). The microanalytical results were found to be reproducible between different preparations of the same compound, and in each case the number of water molecules (n) is given as a best fit to these data. However, the structurally characterized compounds have the same value for n, whether obtained from microanalysis or by X-ray diffraction.

ESR Measurements. Electron spin resonance (ESR) spectra on powdered polycrystalline samples were obtained at X- (ca. 9.25 GHz) and Q-band (ca. 35.0 GHz) frequencies under nonsaturating conditions with a Varian E112 spectrometer. Low-temperature spectra were obtained by using either an Oxford Instruments continuous-flow cryostat (X-band) (77 K) or by immersing the cavity tuning rod in liquid dinitrogen (Q-band) (150 K). The detailed description of the operation of the equipment has been presented elsewhere.[43] All of the spectra presented in Figures 2-12 have an abscissa linear in applied magnetic field in the range 0–20 kG, the form of an individual spectrum at a particular frequency band being unaffected by tuning within the bandwith of the klystron source.

Computation. Computer simulations of ESR spectra were performed by using a previously described program[37] written in FORTRAN and run using large core memory on the Amdahl 470/V7-CDC 7600 computer system at the University of Manchester Regional Computer Centre. Graphical output was obtained from a Benson narrow drum plotter.

Results and Discussion

Structural Considerations. The only published X-ray crystal structure of a complex containing the tris(oxalato)ferrate(III) anion is by Herpin on the tripotassium salt.[44a] It was found that the average chelate O–Fe–O angle was ca. 85° so the structure is very much as would be expected for a tris chelate. The metal is surrounded by a trigonally distorted octahedral array of oxygen atoms in approximate D_3 symmetry, a structure that persists in solution.[45] The parent compound of the malonato series [Co-

(38) Brauer, G. *Handbook of Preparative Inorganic Chemistry*; Academic Press: New York, 1965; p 1516.
(39) Jones, E. M.; Bailar, J. C. *Inorg. Synth.* **1939**, *1*, 36.
(40) Calvert, J. G.; Pitts, J. N. *Photochemistry*; John Wiley and Sons: New York, 1967; p 784.
(41) Ware, M. J. *J. Photogr. Sci.* **1986**, *34*, 13.
(42) Scholz, A. *Monatsh. Chem.* **1908**, *29*, 439.
(43) Collison, D.; Gahan, B.; Mabbs, F. E. *J. Chem. Soc., Dalton Trans.* **1987**, 111.
(44) (a) Herpin, P. *Bull. Soc. Fr. Miner. Cristallogr.* **1958**, *81*, 245. (b) Roof, R. B. *Acta Crystallogr.* **1956**, *9*, 781. Iball, J.; Morgan, C. H. *Acta Crystallogr.* **1967**, *23*, 239.

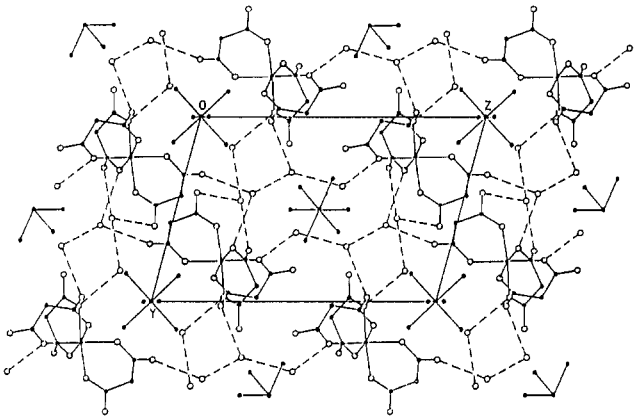

Figure 1. Projection of the crystal structure of $[Co(NH_3)_6][Fe(mal)_3]\cdot 5H_2O$ in the *bc* plane showing the H-bonding network (O---O).

$(NH_3)_6][Fe(mal)_3]\cdot 5H_2O$ has been the subject of an X-ray diffraction study.[46] The anion displays the tris chelate structure expected for this system. Both enantiomers are present in a 1:1 ratio. The unit cell contains two crystallographically independent cations, both displaying inversion symmetry and the expected octahedral geometry. The mean chelate O–Fe–O angle is 87.6° suggesting that the larger chelate ring size leads to a slightly less distorted structure in the complex than in the tris(oxalato) complex. There is an extensive hydrogen-bonding network involving the crystal water molecules and both the bonded and unbonded oxygen atoms of the ligand (see Figure 1).

Hence the distorted octahedral nature of these $\{FeO_6\}$ moieties has been demonstrated by diffraction methods, and the gross structural features of particular salts have been confirmed by comparative vibrational,[47a] electronic absorption,[47b] and Mossbauer[47c] spectroscopies. Thus the two series of complex salts $[Fe(ox)_3]^{3-}$ and $[Fe(mal)_3]^{3-}$ involve the "FeO_6" environment with variables of counterion, degree of hydration, and the possible involvement of steric effects in the chelate rings of tris(malonato) complexes. For any particular compound presented above, the indication of the presence of water(s) of crystallization from microanalysis is seen to be important regarding lattice distortions.

Single-crystal X-ray diffraction studies[44b] have also been reported for the related complex $[Fe(acac)_3]$, which confirm the near-octahedral geometry about the iron atom.

Magnetic Considerations. The room-temperature magnetic moment of the tripotassium salt of the ferrioxalate was found to be 5.75 μ_B by Johnson.[48] This is quite close to the calculated values of 5.92 μ_B expected for a d^5 high-spin ion.[49] Single-crystal magnetic susceptibility measurements, analyzed by assuming axial symmetry, gave D, the axial zero-field splitting parameter, as −0.55 cm^{-1}.[27] Measured values of μ_{eff} at room temperature for the current series of oxalato and malonato salts lie in the range 5.8–6.0 μ_B. The single-crystal ESR spectra obtained when small amounts of the tripotassium salt were doped into diamagnetic hosts, such as tripotassium tris(oxalato)aluminate(III), have been reported.[26] Values for the D and E zero-field splitting parameters are reported to vary depending on the exact nature of cations in the host and the degree of hydration. In their work, McCool and Doetschman used a spin Hamiltonian of the form given in eq 1 for $S = {}^5/_2$. This treatment yielded 14 fine structure parameters and enabled the authors to interpret the observed ESR spectra fully. They concluded that the presence of crystal water in the lattices was important in determining the nature of the ESR spectra, the hydrogen-bonding network playing a major part in creating the distortions evidenced by the zero-field splitting parameters.

Further evidence for the sensitivity of the electronic structure of tris(oxalato)ferrate(III) complexes to the hydrogen-bonding effects of lattice water and to cation dependence is provided by the range of ^{57}Fe Mossbauer isomer shift parameters that have been reported[47,50] for a series of alkali-metal and alkaline-earth-metal salts. The values vary between 0.03 and 0.39 mm s^{-1}, referenced to iron metal.

ESR Spectra. The ESR spectra of six salts of the $[Fe(ox)_3]^{3-}$ anion and five hexamminecobalt salts of anions of the general formula $[Fe\{CR^1R^2(COO)_2\}_3]^{3-}$, and tripotassium tris(malonato)ferrate(III), were measured at X- and Q-band frequencies at room temperature and at 77 or 150 K and are presented in Figures 2 and 3.

In the case of the malonato complexes, the effect of having a hexamminecobalt counterion is to isolate the iron centers, which results in narrower lines due to a reduction in the dipole–dipole interactions and any exchange between the centers.[51] The tripotassium salt shows much broader lines as a consequence of these interactions. The markedly different ESR spectra displayed by these malonato and oxalato complexes, all of which possess the "FeO_6" core, provide insights into the effects of distortion from octahedral geometry. The parameters D and E, obtained by spectrum simulation, can give an indication of the relative distortions in these compounds.

Simulation of Spectra. In order to facilitate the simulation of some of the individual ESR spectra a systematic survey of the effects of D and E at X- and Q-band frequencies was undertaken by using the computer simulation program described previously[37] with a Gaussian line-shape function. In this earlier treatment the experimental Hamiltonian derived from eq 1 was truncated for $n = 2$ as shown in eq 2. This computational method[52] has now

$$\mathbf{H}' = \beta_e \mathbf{B}\cdot\mathbf{g}\cdot\mathbf{S} + D[S_z^2 - S(S+1)] + E(S_x^2 - S_y^2) \quad (2)$$

$$\lambda = E/D$$

been expanded to include additional terms arising from $n = 4$ as shown in eq 3, where a and F are further zero-field splitting

$$\mathbf{H}_{tot} = \mathbf{H}' + (a/_6)[S_2^4 - {}^1/_5 S(S+1)(3S^2 + 3S - 1)] + (F/_{180})[35S^2 - 30S(S+1)S_z^2 - 30S(S+1)S_z^2 + 25S_z^2 - 6S(S+1) + 3S^2(S+1)^2] \quad (3)$$

parameters.[58] For the spin-Hamiltonian of eq 2, when $E = 0$ the system is *axial* and when $\lambda = {}^1/_3$ (or $D = 0$, $E \neq 0$), the

(45) Magini, M. *Chem. Phys. Lett.* **1981**, *78*, 106.
(46) Clegg, W. *Acta Crystallogr., Cryst. Struct. Commun.* **1985**, *C41*, 1164.
(47) (a) Schmelz, M. J.; Nakayawa, I.; Mizushima, S.; Quagliano, J. V. *J. Am. Chem. Soc.* **1959**, *81*, 287. (b) Jorgensen, C. K. *Absorption Spectra and Chemical Bonding in Complexes*; Pergamon Press: Oxford, London, 1962. (c) Brar, A. S.; Randhawa, B. S. *Bull. Chem. Soc. Jpn.* **1981**, *54*, 3166. Brar, A. S.; Brar, S.; Sandhu, S. S. *Polyhedron* **1983**, *2*, 421.
(48) Johnson, C. H. *Trans. Faraday Soc.* **1935**, *31*, 1614.
(49) Figgis, B. N.; Lewis, J. *Prog. Inorg. Chem.* **1964**, *6*, 37.
(50) (a) Gallagher, P. K.; Kurkjian, C. R. *Inorg. Chem.* **1966**, *5*, 214. (b) Brar, A. S.; Randhawa, B. S. *Radiochem. Radioanal. Lett.* **1980**, *44*, 377.
(51) Van Vleck, J. H. *Phys. Rev.* **1948**, *74*, 1168.
(52) We have reconsidered the computational method[37] we used for the simulation of field-swept spectra in the light of the subsequent considerations of Pilbrow et al.,[53,54] which generalized the treatments of Aasa and Vanngard[55] and of Van Veen[56] later employed by Gaffney et al.[57] While the derivation of the expression for first-derivative spectra, assuming Gaussian line shape as a function of applied magnetic field at fixed microwave frequency $\{=dS(\nu_c,B)/dB\}$ from the general expression (eq 8 in ref 53) has been applied successfully by various workers,[54,56,57] it should be noted that two terms in the expansion of $S(\nu,B)\alpha|V_{ij}|^2 f([\nu - \nu_0]^2,\sigma_\nu)$ under these conditions have been considered as unimportant *for the particular system under study*. Thus the general simplifications in proceeding from eq 8 to eq 10 in ref 53 manifest themselves variously as additional terms of reciprocal g dependence, curve-fitting of a line width/shape function and mixed frequency/field expressions. These individual approaches have enabled good fits of spectral band envelopes to be made *within a spectrum for a single fixed microwave frequency*. We have found that application of these and other semiempirical methods does not lead to an improvement in the fits to experimental spectra for data obtained at both X- and Q-band frequencies. In general, however, the method described in ref 37 leads to a good compromise in many cases and is therefore employed in Figures 11 and 12.
(53) Pilbrow, J. R. *J. Magn. Reson.* **1984**, *58*, 186.
(54) Pilbrow, J. R.; Sinclair, G. R.; Hutton, D. R.; Troup, G. J. *J. Magn. Reson.* **1983**, *52*, 386.
(55) Aasa, R.; Vanngard, T. *J. Magn. Reson.* **1975**, *19*, 308.
(56) Van Veen, G. *J. Magn. Reson.* **1978**, *30*, 91.
(57) Yang, A.-S.; Gaffney, B. J. *Biophys. J.* **1987**, *51*, 55.
(58) Vivien, D.; Gibson, J. F. *J. Chem. Soc., Faraday Trans. 2* **1975**, 1640.

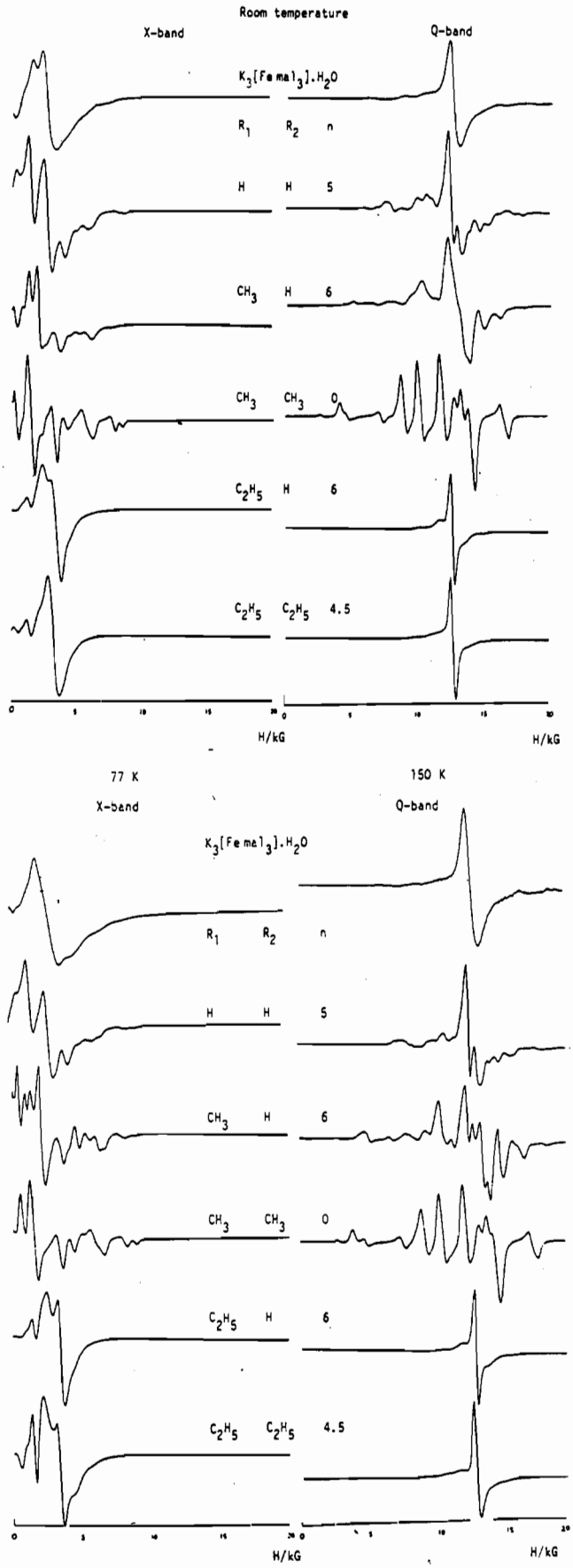

Figure 2. X- and Q-band ESR spectra of $K_3[Fe(mal)_3]\cdot H_2O$ and the series of $[Co(NH_3)_6][Fe\{CR^1R^2C(COO)_2\}_3]\cdot nH_2O$ salts as polycrystalline powders.

system is completely *rhombic*. Therefore the degree of rhombic distortion is indicated by the value of λ. The effects generated for the limiting cases of the allowed values of D, E, a, and F have

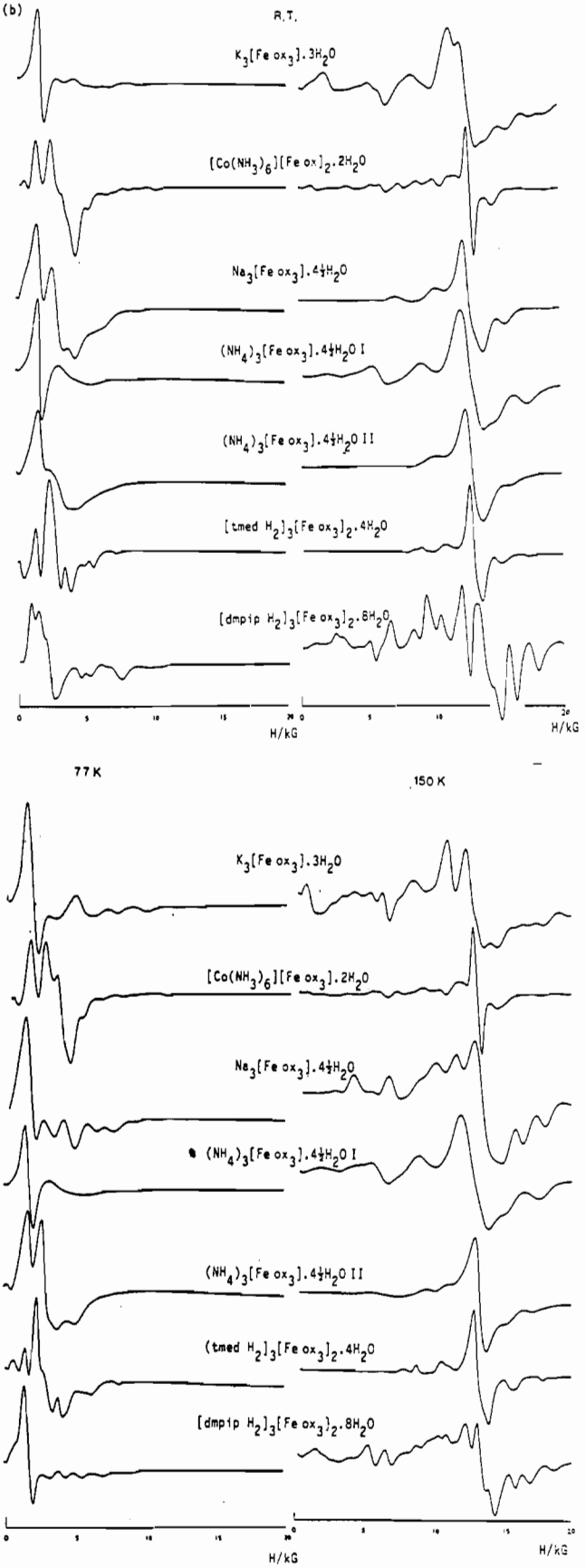

Figure 3. X- and Q-band ESR spectra of a series of $[Fe(ox)_3]^{3-}$ salts as polycrystalline powders.

been reported previously.[59] The effect of varying these Hamiltonian parameters was investigated.[60] Using these simulated

(59) Golding, R. M.; Kestigian, M.; Tennant, C. W. *J. Phys. C* **1978**, *11*, 5041.

spectra as guides, it was then possible to suggest suitable values of D and E as starting points for accurate simulation. This was achieved by considering the possible magnitude of D first (the axial case, corresponding to $E = 0$) by careful comparison of the X- and Q-band spectra and then considering whether or not the system was rhombic ($\lambda = 0$; x and y are inequivalent) and hence involving E.

It is important that both X- and Q-band spectra are considered when using this approach, as it can be difficult to distinguish certain types of spectra when only one frequency is examined. Thus, a strong feature at $g_{eff} = 4.3$ in an X-band spectrum arises in a completely rhombic system ($E/D = {}^1/_3$) for $D > 0.05$ cm^{-1}, but a similar resonance occurs in an axial system when D is large (on the order of 1 cm^{-1}) and the a and F parameters are included in the spin Hamiltonian.[59]

The purpose of simulating the X- and Q-band spectra with a range of D and E values was to make it possible to estimate the magnitude of any zero-field splitting, and as such, it was not necessary (or even possible) to obtain good fits for all the ESR spectra recorded in this work. In fact, it is most unlikely that all the details of a given ESR spectrum can be reproduced by using the simulation method outlined since it was necessary to make the assumption that the zero-field splitting and **g** tensors and the line widths have coincident principal axes in order to perform the calculation in a reasonable time (bearing in mind that the calculation has to take transitions within all three Kramer's doublets into account). While we have restricted the **g** tensor to be isotropic (which, if anisotropic, may indeed be coincident with the zero-field splitting tensor, although it is not *required* to be so), the assumption of anisotropic "tensorlike" behavior for the line-width parameters, where ΔB_i are coincident with g_i, is a convenient computational device only. It is probable that off-axis resonances became apparent in some of the systems studied here, but forearmed with the knowledge of the limitations of the model, it may then be possible to identify absorptions as arising from off-axis components and thus afford an acceptable interpretation of the spectrum.

Lastly, the effect of temperature on the ESR spectra should be considered. Unless the system is antiferromagnetically coupled, or the zero-field splitting is very large, depopulation of higher spin states will not occur on lowering of temperature (i.e. for $T > 10$ K), which means that the ESR spectrum of a given compound should have the same form at room temperature and, for example, 77 K (leaving aside the effect of temperature on relaxation times). However, lowering of temperature can lead to lattice distortions or phase changes, which may in turn alter the magnitude of the zero-field splitting. These effects cannot be predicted by the simulation program; instead, it is necessary to perform a new calculation to determine the zero-field splitting of what is, in effect, a new system.

With these methods of comparing the measured ESR spectra with a series of simulated spectra,[60] it is possible to estimate values of the D (up to ca. 2.0 cm^{-1}) and λ parameters to within ± 0.03 cm^{-1} and ± 0.07, respectively, as estimated from the observed changes in the simulated spectra. All the simulations were performed by taking $g_i = 2$, which is almost always found to be the case in a high-spin d^5 iron(III) system.[27,59]

The values of D and λ that were estimated for the $[Fe\{CR^1R^2(COO)_2\}_3]^{3-}$ and $[Fe(ox)_3]^{3-}$ complexes (whose ESR spectra are shown in Figures 2 and 3) may be found in Table I. In order to demonstrate the fitting procedure, the spectra of $[Co(NH_3)_6][Fe\{C(CH_3)_2(COO)_2\}_3]$ and $(DMPIPH_2)_3[Fe(ox)_3]_2 \cdot 8H_2O$ have been fully simulated by the above computational method,[61]

Table I. ESR Zero-Field Splitting Parameters for Tris Chelate O Donor Iron(III) Complexes Containing the "FeO_6" Core

1. $[Fe(mal)_3]^{3-}$ Complexes with the General Formula $Y[Fe\{R^1R^2C(COO)_2\}_3] \cdot nH_2O$

Y	R^1	R^2	n	D/cm^{-1}	E/cm^{-1}	λ	notes
K_3	H	H	1	0.12	0.032	0.27	*a*
$Co(NH_3)_6$	H	H	5	0.12	0.032	0.27	*a*
$Co(NH_3)_6$	H	CH_3	6	0.14	0.038	0.27	
$Co(NH_3)_6$	CH_3	CH_3	0	0.20	0.0	0.0	*b*
$Co(NH_3)_6$	H	C_2H_5	6	0.045	0.0	0.0	
$Co(NH_3)_6$	C_2H_5	C_2H_5	4.5	0.045	0.0	0.0	

2. $[Fe(ox)_3]^{3-}$ Complexes

formula	D/cm^{-1}	E/cm^{-1}	λ	notes
$K_3[Fe(ox)_3] \cdot H_2O$	0.18	0.055	0.31	*b*
$Na_3[Fe(ox)_3] \cdot 4^1/_2H_2O$ at room temperature	0.14	0.028	0.20	*c*
$Na_3[Fe(ox)_3] \cdot 4^1/_2H_2O$ at 77 K	0.20	0.054	0.27	*c*
$(NH_4)_3[Fe(ox)_3] \cdot 4^1/_2H_2O$, form I	0.20	0.06	0.30	*d*
$(NH_4)_3[Fe(ox)_3] \cdot 4^1/_2H_2O$, form II	0.10	0.02	0.20	*d*
$[Co(NH_3)_6][Fe(ox)_3] \cdot 2H_2O$	0.09	0.024	0.27	
$[TMEDH_2]_3[Fe(ox)_3]_2 \cdot 4H_2O$	0.10	0.02	0.20	*e*
$[DMPIPH_2]_3[Fe(ox)_3]_2 \cdot 8H_2O$	0.20	0.026	0.133	*b*

3. Other "FeO_6" Complexes

formula	D/cm^{-1}	E/cm^{-1}	λ	notes
$[Fe(acac)_3]$	0.14	0.028	0.20	
$[Fe(hydroxybutyrato)_3]$	0.10	0.02	0.20	*e*
$[Fe(ketovalerato)_3] \cdot 2H_2O$	0.08	0.0	0.0	

[a] Line widths are much broader in the case of the K^+ salt. [b] These values have been used to simulate the EPR spectrum. [c] The zero-field splitting of this compound is temperature dependent. [d] This compound appears to crystallize in two different morphologies, giving rise to different degrees of distortion within the lattice and hence zero-field splittings. [e] Although these parameters are the same as for $(NH_4)_3[Fe(ox)_3] \cdot 4^1/_2H_2O$ form II, line-width effects make the spectra appear different.

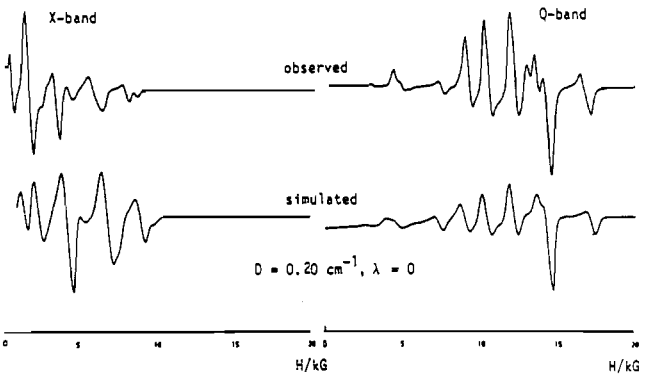

Figure 4. Comparison of computer-simulated ESR spectra with observed spectra of $[Co(NH_3)_6][Fe\{(CH_3)_2C(COO)_2\}_3]$ for a polycrystalline powder.

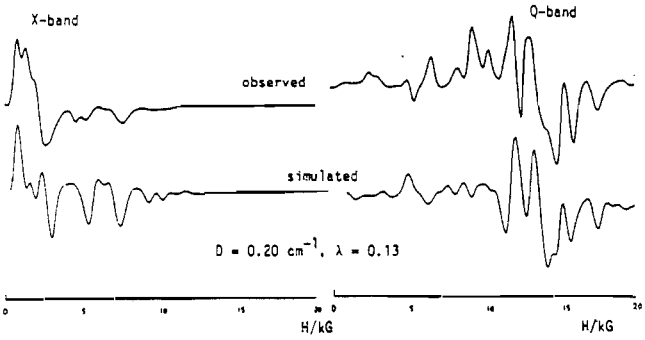

Figure 5. Comparison of computer simulated ESR spectra with observed spectra of $[DMPIPH_2][Fe(ox)_3]_2 \cdot 8H_2O$ for a polycrystalline powder.

and the best fits are shown in Figures 4 and 5. The goodness of fit, as determined by "best fit by eye" between the observed

(60) A systematic study of the variation of the spin Hamiltonian parameters D and E, for fixed values of g_0 (=2.000) and ΔB_0 (=500 G) was undertaken for simulations performed at X- and Q-band frequencies. The results of these calculations form a series of correlation diagrams, which are presented as Figures 11 and 12. The line width was chosen to reflect the apparent breadth of features seen both in the spectra presented in this work and in the spectra of many magnetically undilute materials reported in the literature. The simulation variable $d\theta$ (see ref 37) was decreased for any given simulation until no further gross changes in spectral profile were observed, thus minimizing simulation "noise".

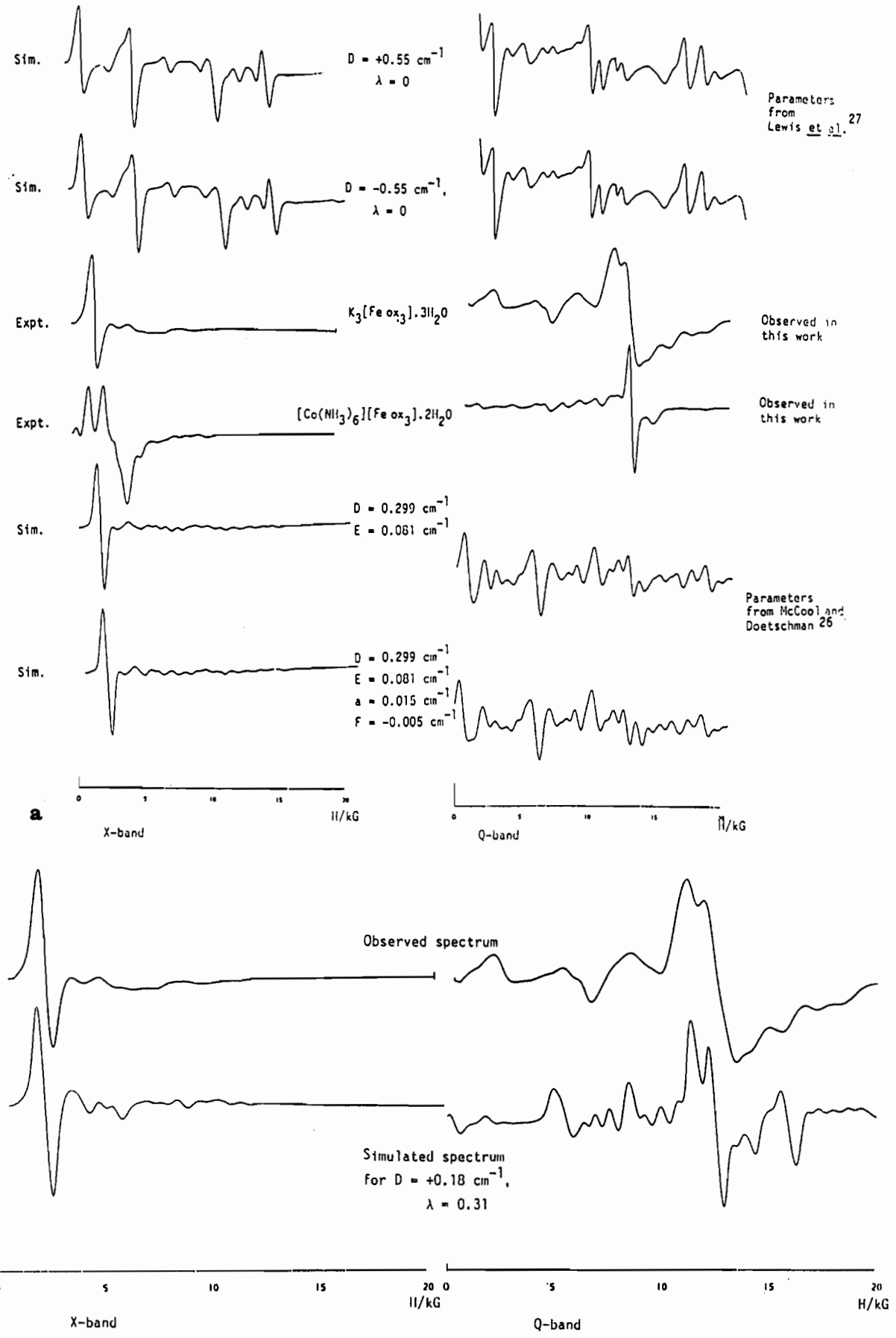

Figure 6. (a) Comparison of methods for obtaining zero-field splitting parameters using $K_3[Fe(ox)_3]\cdot 3H_2O$ as an example, using spectrum simulation procedures. Expt = experimental ESR spectrum; Sim = simulated ESR spectrum. The spectrum of $[Co(NH_3)_6][Fe(ox)_3]\cdot 2H_2O$ is included to show the resonance positions expected for isolated $[Fe(ox)_3]^{3-}$ ions. (b) Comparison of computer-simulated ESR spectra with the observed spectra of $K_3[Fe(ox)_3]\cdot 3H_2O$ for a polycrystalline powder assuming rhombic symmetry.

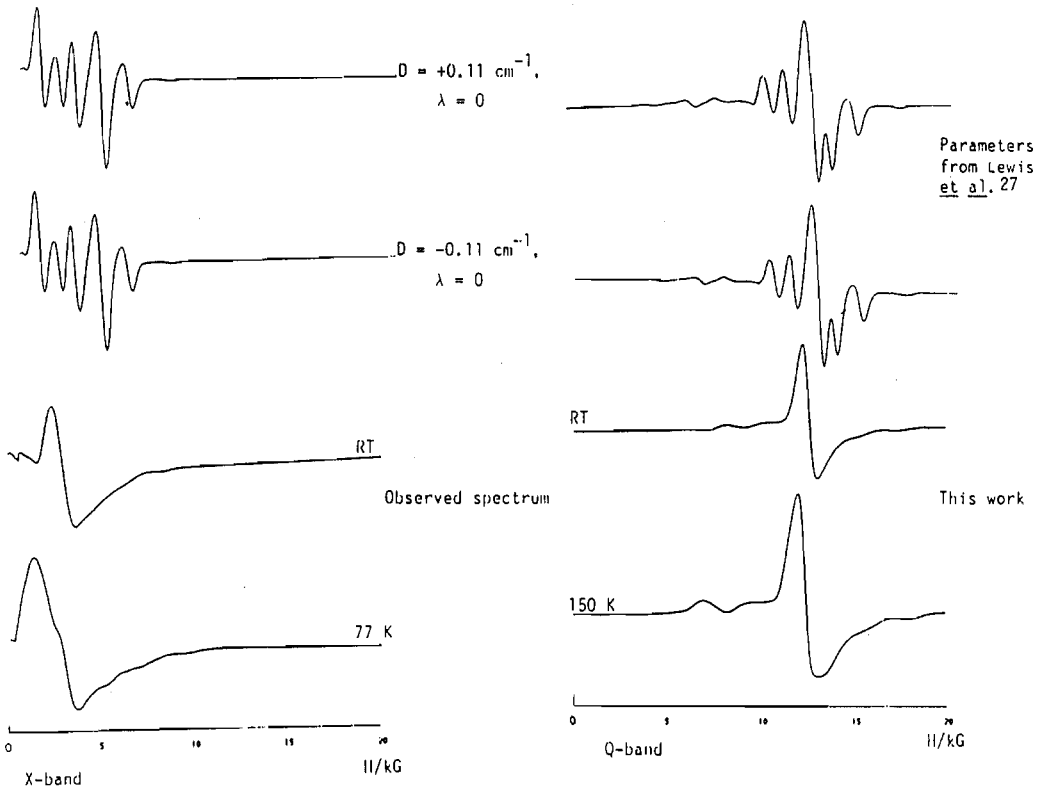

Figure 7. Comparison of the observed spectra of $[Fe(acac)_3]$ with spectra calculated from a literature value of D, the zero-field splitting parameter.

and simulated spectra of Figures 4, 5, and 6b are not of "overlay" quality. From the considerations above (see especially refs 52 and 61), these fits should be viewed in the light of the necessary limitations in the computational procedure employed. In addition, there seems to be no particular value, for the present purposes, in attempting to describe the angular variation of the line width/shape function for these compounds; indeed, this problem will have a nonunique solution given the available experimental data. It is the reasonable agreement between the simulated and measured spectra *at both frequencies* that gives confidence in the values of the simulation variables.

$[Co(NH_3)_6][Fe\{C(CH_3)_2(COO)_2\}_3]$. The EPR spectrum of this complex, measured at X- and Q-band frequencies, is unchanged on cooling the sample from room temperature. Considering the spectra in Figure 4, it can readily be seen that the X- and Q-band spectra with $D = 0.2$ cm^{-1} give an almost perfect fit to the observed spectra, with no apparent rhombic distortion ($\lambda = 0$). This complex might be expected to show an axial rather than rhombic distortion in view of the symmetrically substituted malonate ligands. However, lattice effects are important in determining the nature of the distortion. This can be seen in the case of $[Co(NH_3)_6][Fe\{CH_2(COO)_2\}_3]\cdot 5H_2O$, which has OFeO angles that are all different, as are the individual Fe–O bond lengths, giving rise to a rhombically distorted structure.[46] This type of distortion may be due to the hydrogen-bonding network that is known to exist in the solid state (see Figure 1), or to some constraints of the crystal packing. The value of the zero-field splittings found for the other substituted malonato complexes do not form any logical series, suggesting that lattice effects may be important in determining the degree of distortion from idealized O_h and D_3 geometry.

$[DMPIPH_2]_3[Fe(ox)_3]_2\cdot 8H_2O$. A comparison of the X- and Q-band spectra of this complex with simulations for axially distorted systems[60] shows that the value of D lies in the region of 0.2 cm^{-1}. However, it is apparent that there is a degree of rhombic distortion in this complex. Reference to rhombic spectra[60] with the D value of 0.2 cm^{-1} makes it possible to estimate the size of λ. It is worth pointing out that the variation of λ for a specified D value gives very similar results for nearby D values, and it is not necessary to simulate spectra for small increments in D. From this, λ appears to be 0.133. Simulation of the Q-band spectrum for $D = 0.2$ cm^{-1}, $\lambda = 0.133$ gives a "good fit by eye" to the observed spectrum, as shown in Figure 5. The exact form of the spectrum at X-band frequency is not reproduced, and this may be due to anisotropic line widths in the observed spectrum.

Studies of $K_3[Fe(ox)_3]\cdot 3H_2O$. Two groups of workers have tried to estimate D values from magnetic studies (vide supra). McCool and Doetschman[26] involved the a and F parameters of the general spin Hamiltonian (eq 1) in addition to D (0.299 cm^{-1}) and E (0.081 cm^{-1}) in order to analyze their spectra. When these D and E values are fed into the simulation program, the resulting spectra can then be compared with the ESR spectra recorded in this work. The Q-band spectrum of $K_3[Fe(ox)_3]\cdot 3H_2O$ is quite unusual and rather characteristic (whereas the X-band spectrum is not) and the Q-band frequency was chosen for the comparisons, which are shown in Figure 6. The D value of –0.55 cm^{-1} suggested by Lewis

(61) There appears to be no general agreement in the literature among workers who require field–frequency interconversions derived for multielectron ESR spectroscopy, whether they are empirical or semiquantitative treatments (compare, for example, the frequency/field equations of Gaffney[57] et al., the parametrized approach of Pilbrow[62] et al., with the use of statistical density functions and parameterisation of Stevenson[63] and interpolation of field-dependent quantities in the early treatment due to Coffmann[64]). It is not our intention to use the data in this paper to address further these difficulties. Indeed, the use of powder spectra for that purpose is likely to confuse the deconvolution of line width/line shape/transition probability factors. It should, however, be noted that data obtained over a wide field range and at two disparate microwave frequencies (see for example Figure 5) are not readily treated by a single frequency–field conversion (data not shown) and therefore suggests a reexamination of the assumptions inherent in eq 10 of ref 53 may be undertaken, when data of sufficient quality and diversity become available. *Pilbrow[65] has recently reported the true nature of the 1/g "correction" factor and along with Gibson[66] confirms that its use in spectrum simulation is unnecessary.* We stress that it is the intention of this paper to present a "library" of real examples of high-spin Fe(III) ESR spectra, where the semiquantitative description of the deviation from an ideal "FeO_6" octahedron may be described with recourse to multifrequency comparisons as well as spectrum simulation.

(62) Sinclair, G. R.; Pilbrow, J. R.; Hutton, D. R.; Troup, G. J. *J. Magn. Reson.* **1984**, *57*, 228.

(63) Stevenson, R. C. *J. Magn. Reson.* **1984**, *57*, 24.

(64) Coffman, R. E. *J. Phys. Chem.* **1975**, *79*, 1129.

(65) Pilbrow, J. R. *Bull. Magn. Reson.* **1988**, *10*, 32.

(66) Gibson, J. F. *Electron Spin Resonance*: Specialist Periodical Report IIB; Royal Society of Chemistry: London, 1989; p 24.

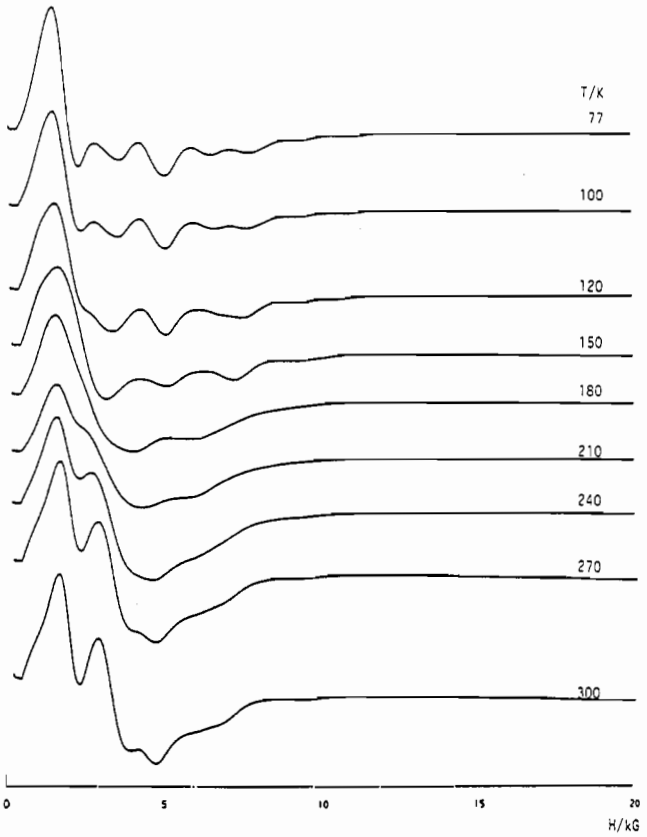

Figure 8. Variation of the X-band ESR spectrum of a polycrystalline powder of $Na_3[Fe(ox)_3]\cdot4^1/_2H_2O$ with temperature.

et al.[27] does not come close to reproducing the observed ESR spectrum. Lewis et al.[27] proposed a negative D value on the basis of crystal field considerations. The D values obtained from ESR studies may be either positive or negative. Simulation of both positive and negative values gives rise to identical spectra for the same D as shown in Figure 6.

There is also no agreement with the experimental spectrum when the values suggested by McCool and Doetschman[26] are used. Simulations of the spectra with D, E, a, and F parameters as well as the D and E parameters alone were tried as indicated in Figure 6. The minor differences observed when $a = F = 0$ serve to reinforce the suggestion[52] that it is unlikely that effects due to small nonzero higher order terms ($C_{nm}O_n$ where $n = 4$, $m = 0$, 2, 4) to the spin Hamiltonian of eq 1 will be detected from powder spectra. The lack of success in transferring spin-Hamiltonian parameters between single-crystal and polycrystalline powder data in this case seems to indicate that the isolation of the iron centers and the effects of hydration and crystal packing does not afford a generally applicable method of analysis. The results of a "best fit by eye" simulation are given in Figure 6b, where the positions of spectral features and their general shapes are reproduced adequately after consideration of the limitations of simulation methods (see above).

A further example of "FeO_6" tris chelate coordination is furnished by the well-characterized $[Fe(acac)_3]$ complex. Single crystals of this compound were also studied by Lewis et al.[27] using the magnetic anisotropy method. Data for this complex are presented here for comparative purposes in Figure 7. The value of D of -0.11 cm^{-1} derived from the magnetic susceptibility studies clearly fails to reproduce the observed ESR spectrum obtained for this compound.

$Na_3[Fe(ox)_3]\cdot4^1/_2H_2O$. Reference to Figure 2 shows that the X-band spectrum of the title complex changes radically when the sample is cooled from room temperature to 77 K. The different spectra can be individually interpreted, for example with $D = 0.14$ cm^{-1}, $\lambda = 0.20$ at room temperature and $D = 0.20$ cm^{-1}, $\lambda = 0.27$ at 77 K. The rather smooth transformation of the spectrum with temperature (see Figure 8), which was found to be reversible,

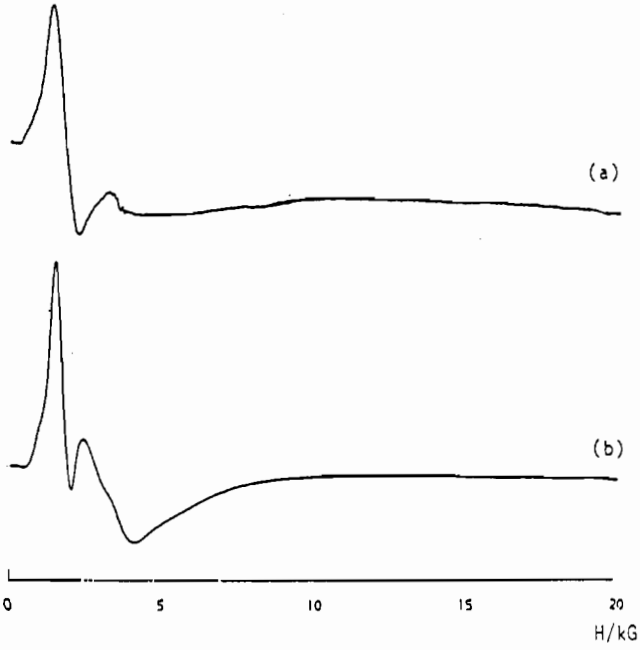

Figure 9. Frozen aqueous solution spectra of (a) $[Fe(ox)_3]^{3-}$ and (b) $[Fe(mal)_3]^{3-}$ at X-band frequency at 77 K.

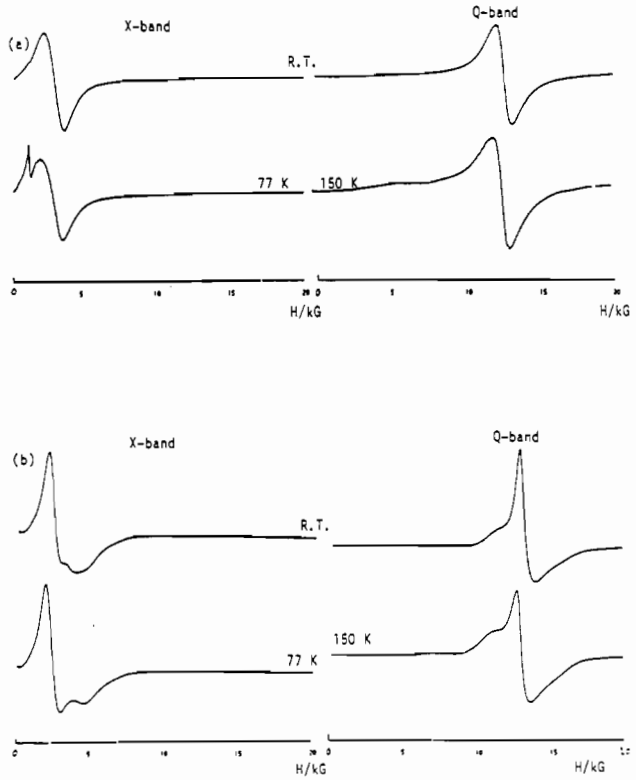

Figure 10. X- and Q-band ESR spectra of (a) $[Fe(ketovalerato)_3]\cdot2H_2O$ and (b) $[Fe(hydroxybutyrato)_3]$ as polycrystalline powders.

suggests a gradual lattice distortion of a rhombic nature, since the values of both D and λ increase on cooling.

This is the only $[Fe(ox)_3]^{3-}$ salt to show such a large change in zero-field splitting at different temperatures, and it has been possible to interpret the ESR spectra of all the other salts by using the same D and λ values for room temperature and 77 or 150 K. In the case of $Na_3[Fe(ox)_3]\cdot4^1/_2H_2O$, variation of D and λ with temperature is a significant effect since D is of sufficient magnitude to give rise to characteristic X- or Q-band spectra;[60] i.e., it would be possible to miss this effect in other systems.

Frozen-Solution Spectra of $[Fe(mal)_3]^{3-}$ and $[Fe(ox)_3]^{3-}$. The X-band ESR spectra of frozen aqueous solutions containing $[Fe(mal)_3]^{3-}$ and $[Fe(ox)_3]^{3-}$ are shown in Figure 9. The two

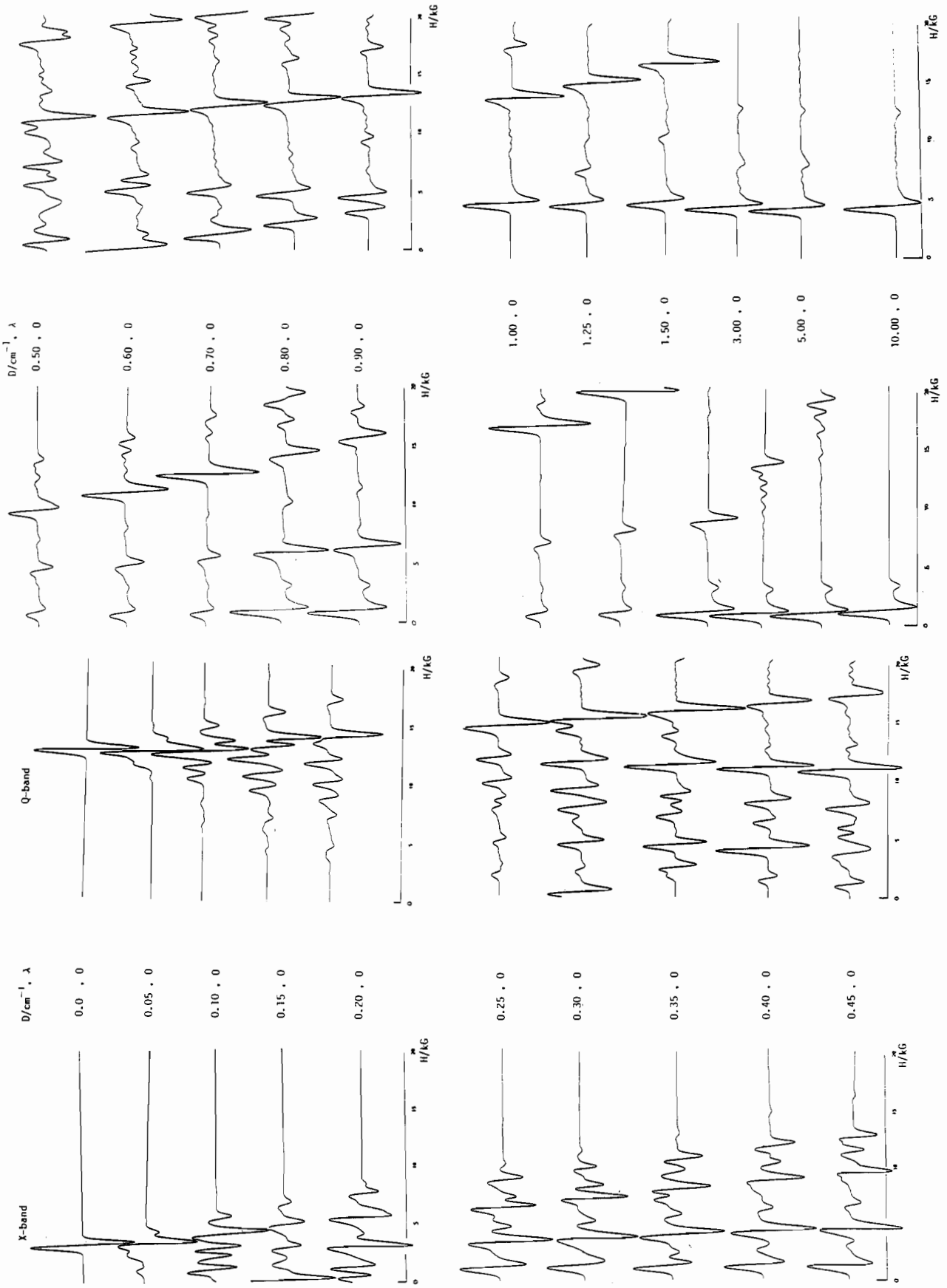

Figure 11. Computer simulations of X- and Q-band spectra with $D = 0$ to 10 cm^{-1} (axial).

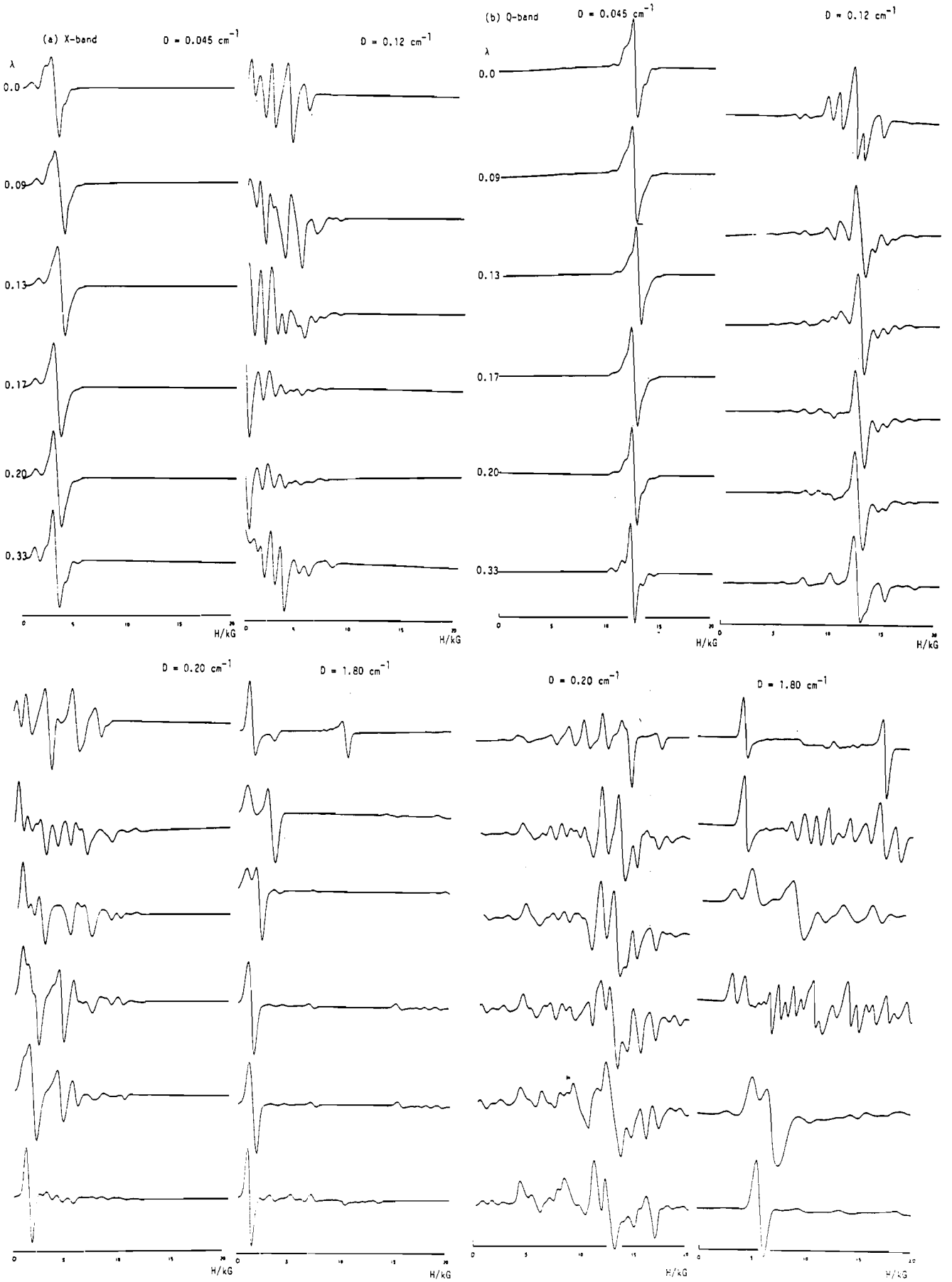

Figure 12. Computer simulation of (a) X-band and (b) Q-band spectra showing the effect of λ ($\lambda = 0$–$^1/_3$) for selected D values (rhombic).

spectra are very similar and show resonances at ca. 1.65 and ca. 3.3 kG only, corresponding to $g_{eff} = 4.3$ and $g_{eff} = 2.0$, respectively. This demonstrates that both $[Fe(mal)_3]^{3-}$ and $[Fe(ox)_3]^{3-}$ are rhombically distorted in solution ($\lambda = 0.3$), which shows that many of the features observed in the polycrystalline powder spectra of salts of these complexes arise from lattice effects.

Summary. The complexes considered can be divided into three groups with one complex in each group having been crystallo-

graphically characterized. All the structure are known to have the iron(III) ion surrounded by an octahedral array of oxygen atoms, yet no two complexes appear to give rise to the same set of ESR spectra. This is due to small distortions in the bond lengths and angles about the iron(III) ion, which can be explained for any one ligand type in terms of lattice effects and hydrogen bonding arising from the interaction of lattice water with the ligands attached to the metal.

The three groups of complexes are given below together with a summary of their ESR characteristics.

1. Complexes of general formula $[Fe\{CR^1R^2(COO)_2\}_3]^{3-}$ were studied. A series of hexamminecobalt salts of these complexes were investigated and showed that the nature of R was not as important as the degree of hydration and presumably hydrogen bonding in determining the magnitude of the zero-field splitting parameters D and E.

2. A series of salts of the $[Fe(ox)_3]^{3-}$ complex was investigated. These compounds have D values of between 0.1 and 0.2 cm^{-1}, which allows the effects of changes in λ to be investigated via their ESR spectra since for these D values the spectra have been shown to be sensitive to small changes in λ. The ESR spectra again demonstrate the importance of lattice effects with regard to distortions from octahedral geometry.

3. The polycrystalline powder ESR spectra of all the neutral tris chelates $[Fe(acac)_3]$, $[Fe(CH_3CH_2CH_2COCO_2)_3]$, and $[Fe\{CH_3CH_2CH(OH)CO_2\}_3]$, display very broad lines (see Figures 7 and 10) presumably because of the lack of counterion, and consequently, spectra of this sort cannot easily be interpreted beyond estimating the probable size of any axial or rhombic distortion. $[Fe(acac)_3]$ displays the best resolved spectra of this set of complexes and a significant degree of rhombic distortion with estimated zero-field splitting parameters of $D = 0.15$ cm^{-1}, $\lambda \simeq 0.3$, which are clearly temperature dependent (see Figure 7). The two carboxylato complexes would appear to have similar values of D and λ.

The ESR spectra can be interpreted in terms of the zero-field splitting parameters D and λ by using a computer-simulation technique. It has been shown that this method is preferable to methods such as anisotropic susceptibility studies and doping of complexes into diamagnetic hosts for determining the values of D and λ. This is due to the limitations of the susceptibility studies and the effect of site symmetry and hydration of the host lattice on the observed ESR spectrum, respectively.

From these studies, it is concluded that three main factors determine the degree of distortion in "FeO_6" complexes. First the amount of water present in the lattice is important. Not only do the water molecules form part of a hydrogen-bonding network in hydrated crystals but also the number of water molecules per iron(III) is significant. Second, the counter-ion can affect the form of the lattice and hence any zero-field splitting. This effect is hard to separate from the effects of hydration mentioned above. Last, there are the packing forces to consider: these are probably responsible for the rhombic distortion observed in the case of the $[Fe(acac)_3]$ complex, which has neither lattice water nor counterions to account for the significant zero-field splitting and yet has a nearly ideal O_h environment.

Conclusion

Our approach to the problem of rationalizing the ESR spectra of spin systems for which $S > {}^1/_2$ has enabled us to interpret the powder spectra of $S = {}^5/_2$ (d^5) systems using the spin-Hamiltonian parameters D and E. All previously reported attempts have been limited to interpreting the spectra of individual (or a few) complexes, and in many cases, it is possible that either by the use of only one frequency to record the spectra or by using an oversimplified approach (whereby an axial geometry is imposed on a rhombic system) the true features have been missed. The ESR spectra of any high-spin iron(III) system can have any one of a huge variety of spectral patterns made possible by very small changes in geometry about the Fe center caused by lattice distortions, solvent molecules, counterions, or any combination of these. It is easy to be confused by using the relatively few examples at present available in the literature and especially if the sample(s) under study are powderlike undiluted materials.

It should be noted that the multifrequency approach reported herein does not demand the use of single crystals of the material under study, thus making the methods particularly applicable to measurements on metallobiomolecules. This work is of particular relevance to the study of $\{FeO_6\}$ sites such as those found in siderophores, for example enterobactin,[2] and especially to compare with recent results published on transferrins.[67] We have demonstrated that a wide variety of ESR spectral patterns is possible and does occur for $S = {}^5/_2$ spin systems and have created a fingerprint library that should be of use to workers in this field, especially with regard to gauging the degree of distortion from idealized geometries about the central metal atom. Hence comparisons of ESR spectral type from an "unknown" system may allow a semiquantitative description of any deviations from ideal geometry.

Acknowledgment. We thank the SERC, U.K., and The Royal Society (D.C.) for financial support and the University of Manchester for the provision of a studentship to A.K.P. We acknowledge helpful discussions with Drs. F. E. Mabbs and M. J. Ware.

(67) (a) *Proceeding of the 6th International Conference on Structure of Functional Iron Storage Transport*; Urushizuki, I., Aisen, P., Listowsky, I., Eds.; Elsevier: Amsterdam, 1983. (b) Aisen, P.; Leibman, A.; Zweier, J. *J. Biol. Chem.* **1978**, *253*, 1930.